

## Supporting Information

### **Kinetic reconstruction of TiO<sub>2</sub> surfaces as visible-light-active crystalline phase with high photocatalytic performance**

Peng Zheng,<sup>1,2</sup> Ruipeng Hao,<sup>1,2</sup> Jianghong Zhao,<sup>1</sup> Suping Jia,<sup>1</sup> Baoyue Cao,<sup>1,2</sup> Zhenping Zhu<sup>\*,1</sup>

<sup>1</sup>State Key Laboratory of Coal Conversion, Institute of Coal Chemistry, Chinese Academy of Sciences, Taiyuan 030001, China

<sup>2</sup>University of Chinese Academy of Sciences, Beijing, 100049, China

This suppling information contains experimental details, Figures S1-S7.

### **1. Experimental details:**

#### **1.1. Reconstruction of TiO<sub>2</sub> nanoparticles**

Commercial P25 was employed as original TiO<sub>2</sub> nanoparticles and trinitrophenol (TNP, analytical grade) was used as explosive substance. In the typical experiments, 2.5 g of P25 and 1.63 g of TNP were physically mixed and fed into a sealed stainless steal reactor (Figure S1). When the reactor was heated to about 310 °C in a tubular furnace, TNP decomposed explosively (at a microsecond time scale) and produced huge heat and a lot of gases (CO, CO<sub>2</sub>, N<sub>2</sub> and H<sub>2</sub>O as revealed by gas chromatography), which created much quickly (about 1 second) a high-temperature and high-pressure environment within the reactor, typically about 950 °C and 4.3 MPa (balance pressure). During the explosive decomposition of TNP, the co-existing TiO<sub>2</sub> nanoparticles would be bombed by the produced high-pressure hot gases and tended to

transform in their structure. Just after the TNP explosion, the reactor was taken out the furnace immediately (within 5 seconds) to allow it cool quickly in air, by which the surface disordered  $\text{TiO}_2$  (SD- $\text{TiO}_2$ ) with black color was obtained after the reactor was cooled to room temperature and the gaseous products were discharged. The surface reconstruction  $\text{TiO}_2$  (SR- $\text{TiO}_2$ ) was obtained when the reactor was allowed stay in the hot furnace for more than 10 minutes to slow down the rate of the heat release inside reactor, by which the original  $\text{TiO}_2$  nanoparticles would undergo an additional annealing process.

## 1.2. Sample analyses

The crystalline structures of the samples were analyzed by X-ray diffraction using a Rigaku X-Ray Diffractometer equipped with a Cu  $\text{K}\alpha$  X-ray source. TEM (HRTEM) images were taken using a JEM2100 transmission electron microscope. Specimens were prepared for TEM by ultrasonically dispersing the sample in ethanol and dropping the obtained suspensions onto a carbon-coated copper grid. Chemical composition and valence analysis of the samples were performed using X-ray photoelectron spectroscopy (ULVAC-PHI5000, a monochromatic Al  $\text{K}\alpha$  X-ray source). Binding energies were referenced to the C 1s peak (284.6 eV) arising from adventitious carbon. UV-vis absorption spectra of the samples were obtained on a UV-vis spectrometer (UV3600, Shimadzu, Japan), using dry-pressed disk samples and a diffused reflectance mode.  $\text{BaSO}_4$  was used as a reflectance standard in the measurements. Raman spectra of the samples were recorded at room temperature with a JYH2800 micro-Raman system equipped with a 532 nm Ar ion laser. EPR was measured using a JEOL, JES-RE2X electron spin resonance spectrometer, conducted at power 1 mW and amplitude  $2.5 \times 100$  at room temperature, without illumination.

## 1.3. Photoelectrochemical characterizations

Photoelectrochemical (PEC) experiments were carried out using CHI760E

workstation (CH Instruments) in a standard three-electrode electrochemical cell configuration under the irradiation of a 300W xenon lighter with a cut-off filter ( $\lambda > 420$  nm). 1 M NaOH solution was used as the electrolyte. The working electrode was 5 mg of photocatalysts dispersed within a surface area of 0.3 cm<sup>2</sup>. Platinum wire (99.9%) was used as the counter electrode, and Ag/AgCl electrode was used as the reference electrode.

#### **1.4. Photocatalytic Activity Tests**

Photocatalytic reactions were conducted in a closed gas-circulation reaction system. The photocatalyst powder (0.05 g) was dispersed using a magnetic stirrer in an ethanol aqueous solution, 100 ml, containing 20% ethanol. The photocatalytic system was illuminated from the top window (flat quartz) of a Pyrex reactor. The reaction was carried out by irradiated with visible light ( $\lambda > 420$  nm) through a cutoff filter from a 300-W Xe lamp (Beijing Trusttech Co. Ltd, PLS-SXE-300UV). The amount of H<sub>2</sub> evolved was measured by an online gas chromatography (Beifen-Ruili: SP-2100, MS-5Å column, TCD, Ar carrier). Note that the loading of cocatalyst platinum on TiO<sub>2</sub> surfaces was conducted by an in situ photo-deposition method with H<sub>2</sub>PtCl<sub>6</sub>·H<sub>2</sub>O solution, referring to the literature (Herrmann, J. M., Disdier, J. & Pichat, P. Photoassisted platinum deposition on TiO<sub>2</sub> powder using various platinum complexes. *J. Phys. Chem.* **90**, 6028-6034).

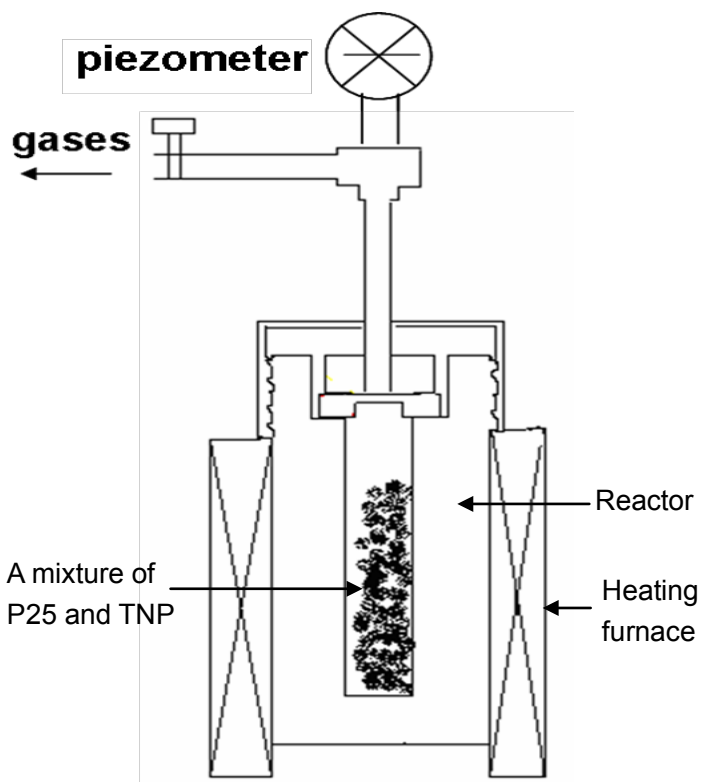


**Figure S1.** Schematic of the stainless steel reactor for the reconstruction of  $\text{TiO}_2$  nanoparticles by a bombardment with high-pressure hot molecules produced from the explosive decomposition of TNP. The inner volume of the reactor is 14 ml.

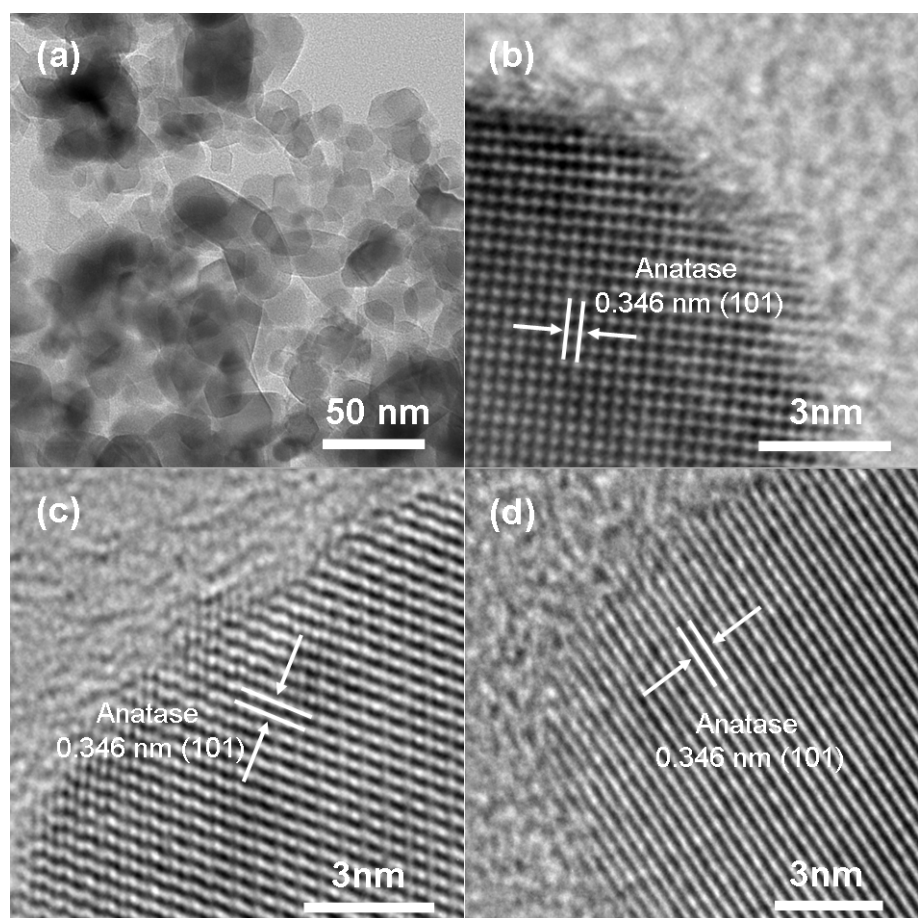


**Figure S2.** TEM images of the original  $\text{TiO}_2$  nanoparticles (P25). (a) A typical low-resolution image. (b-d) High-resolution images show that anatase crystals are dominant and that their surfaces are well crystallized, with space lattice consecutively integrating with the bulk ones.

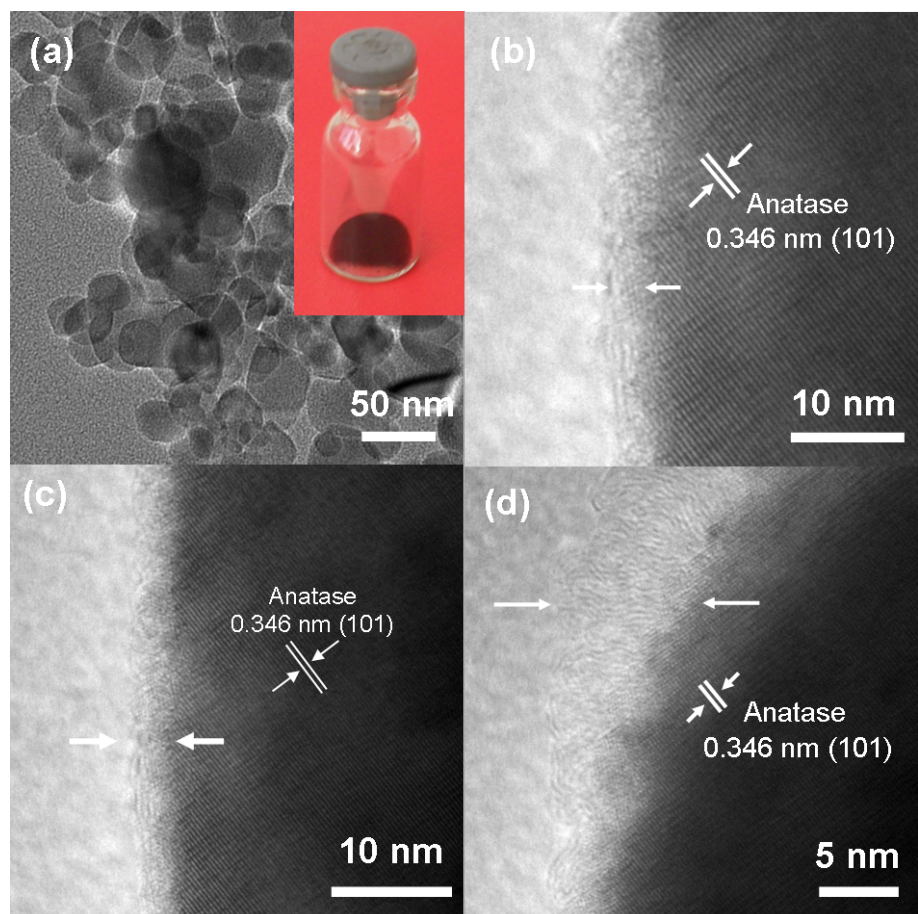


**Figure S3.** TEM images of the black sample (SD-TiO<sub>2</sub>) obtained from a quick cooling behind the hot molecule bombardment. (a) A typical low-resolution image. The inset shows the photograph of the sample, which displays a black color. (b-d) The high-resolution images show the formation of disordered layers on the surfaces of anatase TiO<sub>2</sub> crystals.

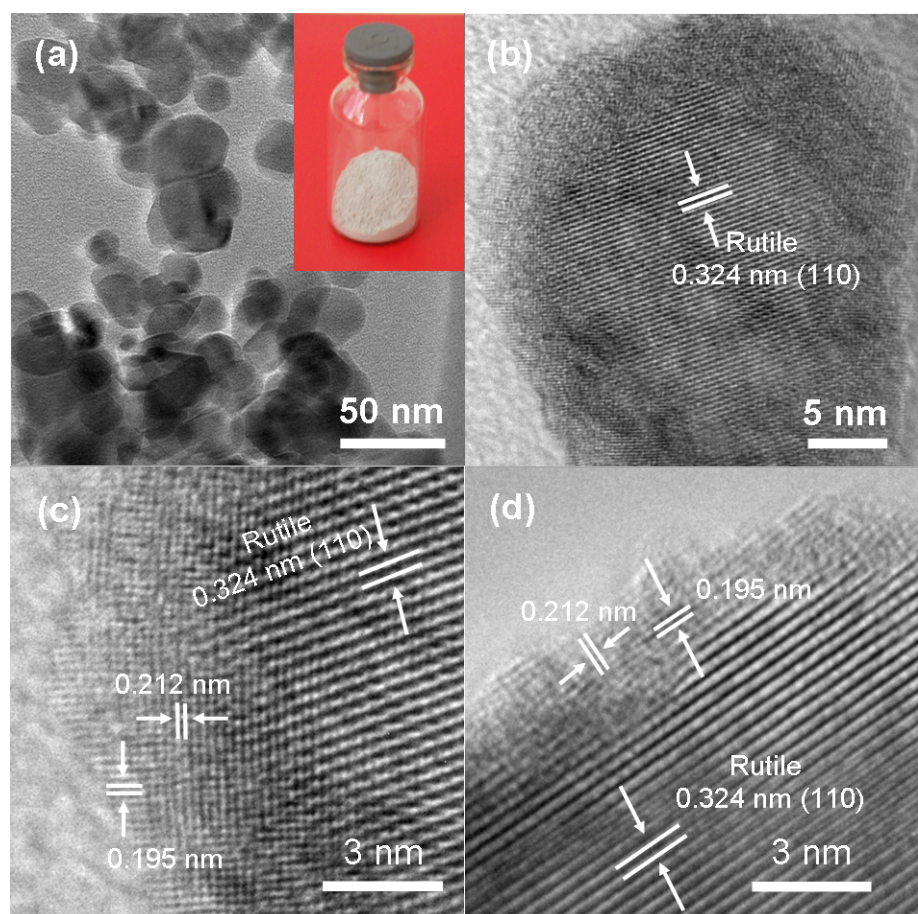


**Figure S4.** TEM images of the light-gray sample ( $\text{SR-TiO}_2$ ) obtained from a slow cooling behind the hot molecule bombardment. (a) A typical low-resolution image. The inset shows the photograph of the sample, which displays a light-gray color. (b-d) The high-resolution images show the formation of a new crystalline phase on the surfaces of rutile  $\text{TiO}_2$  crystals.

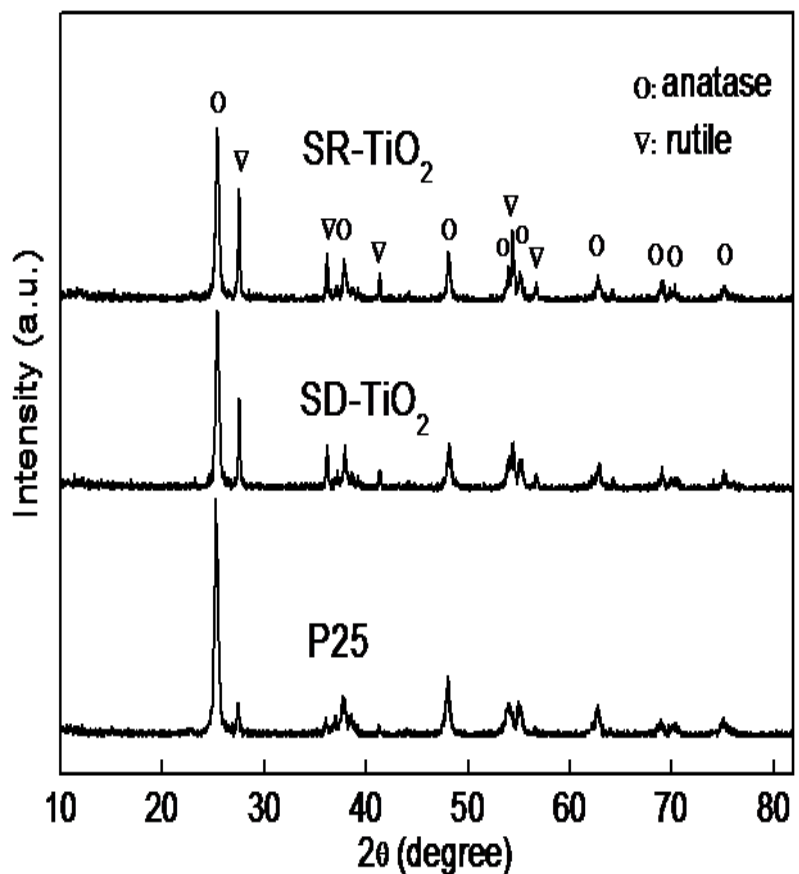


**Figure S5.** X-ray diffraction patterns of P25, SD-TiO<sub>2</sub> and SR-TiO<sub>2</sub>, which show that only anatase and rutile phases are observed in the samples and that the ratio of rutile to anatase phase significantly increase in the order of P25, SD-TiO<sub>2</sub> and SR-TiO<sub>2</sub>, reflecting different-degree bulk phase transformations from anatase to rutile induced by the hot molecule bombardment. Note that the new crystalline surface phase in SR-TiO<sub>2</sub> observed by HRTEM and Raman spectrum showed no XRD signal, possibly due to its small sizes (< 3 nm normally).

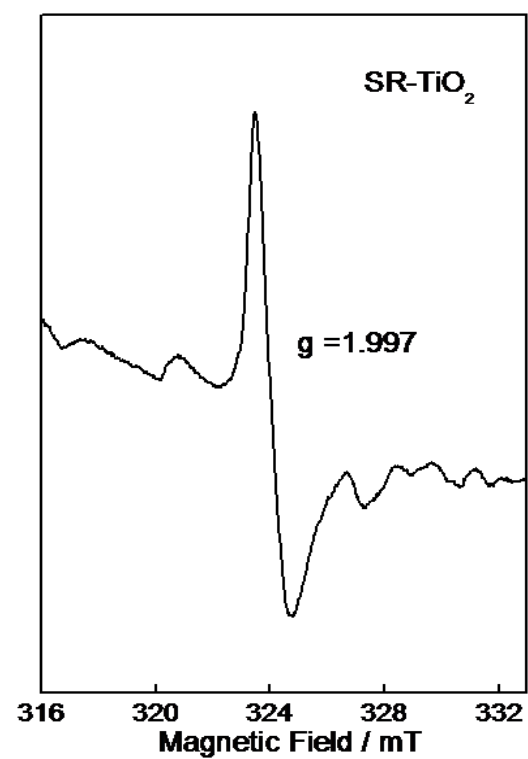


**Figure S6.** EPR spectrum of the SR-TiO<sub>2</sub> shows a resonance signal at  $g = 1.997$ , suggesting the existence of paramagnetic Ti<sup>3+</sup> species.

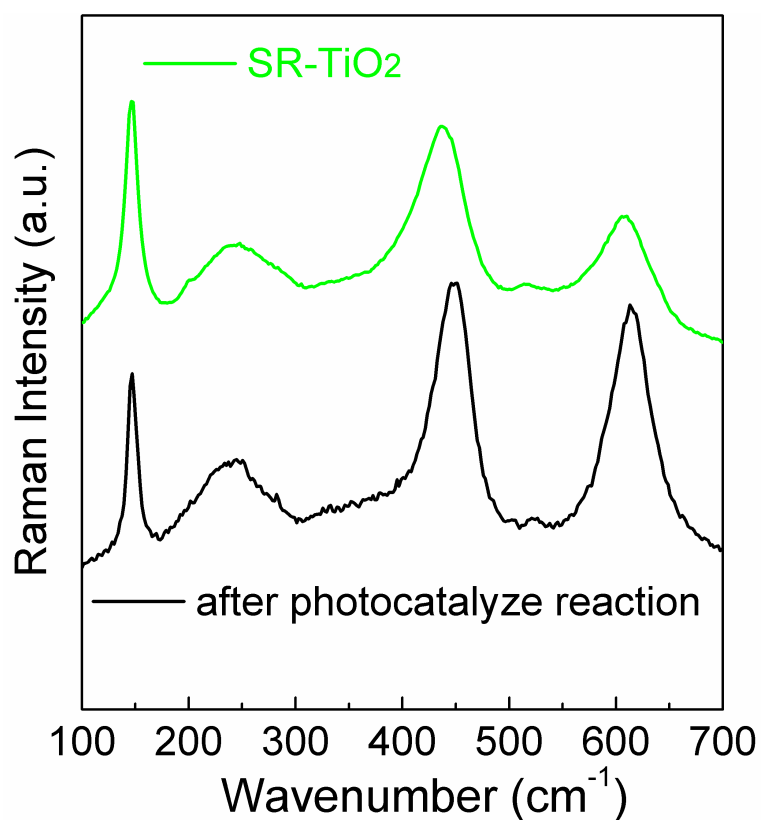


**Figure S7** Raman spectra of SR-TiO<sub>2</sub> and the curves of SR-TiO<sub>2</sub> after photocatalytic hydrogen production reaction.